

Effect of Higher-Order PSDs on Timing Jitter

Isamu Wakabayashi*, Daisuke Abe*, Masatoshi Sano*

*Faculty of Engineering, Tokyo University of Science, 1-14-6 Kudan-kita, Chiyoda-ku, Tokyo Japan 102-0073

wakaba@ee.kagu.tus.ac.jp

Abstract— This paper describes the effect of higher-order PSDs at a squarer output on the jitter variance at a timing circuit output. The timing circuit consists of a squarer, a pre-filter, and a PLL arranged in tandem. The transmission schemes are assumed to be PAM, ASK and QAM. Additive white Gaussian noise exists at the receive filter input. The band-limiting scheme is assumed to be of a cosine roll-off. The higher-order PSDs are components of the jitter source PSD at the squarer output. Theoretical calculations show that the SS and SN components of the jitter source PSD can be represented by 0th- and ± 2 nd-order PSDs. However, based on numerical calculations, the SN component consists of only the 0th-order PSD. This may be due to the effect of the band-limiting scheme assumed herein. The results hold for all of the transmission schemes, SNRs, alphabet sizes, and roll-off factors treated in this paper.

Keywords— Timing jitter, Higher-order PSDs at the squarer output, PAM, ASK, QAM

I. INTRODUCTION

This paper presents the effect of higher-order power spectral densities (PSDs) on jitter variance. The higher-order PSDs are the components of jitter source PSD at the squarer output in a timing circuit consisting of a squarer and a PLL.

The timing jitter due to self-noise in the case of a timing circuit consisting of a non-linear device and a PLL is treated for a noiseless PAM system in [1][2][3]. In [4], a timing extraction algorithm denoted as the Square-Law Nonlinearity is provided based on maximum likelihood estimation at a low SNR for linear modulations, since low SNR operation is performed according to the circumstances. In [5], for baseband polar system, BPSK, and QPSK with additive white Gaussian noise at the receive filter input, timing jitter was analyzed with a timing circuit consisting of a squarer and a narrow band BPF and a representation for jitter PSD was derived. In [6], for PAM, ASK, and QAM with additive white Gaussian noise, analysis of timing jitter was performed for the case of a timing circuit consisting of a squarer and a PLL, which resulted in a general expression for a jitter PSD being derived. In the expression, the jitter PSD is described as a linear combination of the jitter source PSD and the extractor transfer characteristics. The jitter source PSD has SS, SN, and NN components. The SS component is caused by the cross product of the signal with itself and is often referred to as the self-noise or pattern jitter [1]. The SN component is caused by

the cross product of the signal and the noise, and the NN component is caused by the cross product of the noise with itself. The SS and SN components of the jitter source PSD are represented as sums of higher-order PSDs in theoretical calculations, whereas the NN component does not have any higher-order PSDs, because it originates from the additive Gaussian noise. Each component of jitter variance at a PLL output can be calculated by frequency integration of the corresponding component of the jitter PSD over a finite frequency domain.

Based on the general expression in [6], we have presented and discussed dependencies of design parameters such as SNR, alphabet size, transmission scheme, PLL normalized noise bandwidth, and roll-off factor on timing jitter showing some numerically calculated examples [7][8]. In addition, we have presented and discussed the effect of a pre-filter on jitter variance [9]. In the present paper, we consider that it is important to examine the effect of the higher-order PSDs on jitter variance in order to grasp concretely jitter performance, because the jitter source PSD is given as a sum of higher-order PSDs.

II. ASSUMPTIONS

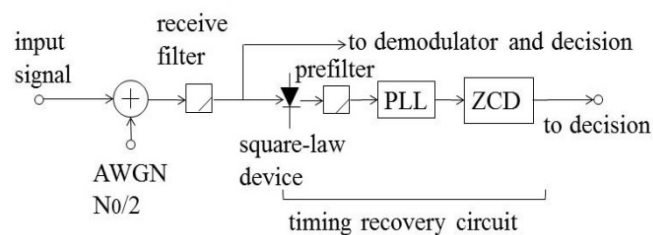


Figure 1. Receiver Configuration

Figure 1 shows the receiver configuration. The timing circuit consists of a square-law device (referred to as a squarer), a pre-filter, a PLL and a zero crossing detector (ZCD) arranged in tandem. The ZCD generates pulse waveforms at the zero crossings of the sinusoidal wave at the PLL output. A randomly modulated signal with additive white Gaussian noise is applied to the receive filter input. A signal and noise composite waveform at the squarer output can be decomposed into a deterministic component and a random component. The

timing wave and the random component pass through the extractor that includes the pre-filter and the PLL. Thus, the sinusoidal wave appears at the PLL output. The phase of the sinusoidal wave fluctuates due to the random component. This fluctuation is referred to as timing jitter.

The transmission schemes are assumed to be PAM, ASK, and QAM. A band-limiting scheme is assumed to be of a cosine roll-off, where the roll-off factor is assumed to be from 0.1 to 1.0. The pre-filter transfer function is assumed to be unity for simplicity herein. The PLL is assumed to be of second order, and its loop filter is assumed to be an active filter. The damping factor, ζ , is assumed to be $\zeta = 1/\sqrt{2}$. The PLL normalized noise bandwidth $b_L = B_L T = 2\pi B_L / \omega_r$ is assumed to range from 10^{-4} to 10^{-2} . Here, B_L is the PLL one-sided noise bandwidth, T is the symbol period, and ω_r is the clock radian frequency. The modulation data a_n and b_n are assumed to be i.i.d. random variables that take M values between $\pm(M-1)$, where M is an alphabet size.

III. REPRESENTATIONS of HIGHER-ORDER PSDS

The general expression for jitter PSD has been presented in [6]. We have adjusted the expression in order to satisfy the assumptions herein. The result expresses the jitter source PSD as a sum of higher-order PSDs as in equations (1), (2), and (3).

$$W_z(\omega) = k_1 W_{z1}(\omega) + k_2 W_{z2}(\omega) + k_3 W_{z3}(\omega) + k_4 W_{z4}(\omega), \quad (1)$$

$$W_{zp}(\omega) = (1/4) \left\{ W_{Rp}^{(0)}(\omega - \omega_r) + W_{Rp}^{(0)}(\omega + \omega_r) - W_{Rp}^{(-2)}(\omega - \omega_r) - W_{Rp}^{(2)}(\omega + \omega_r) \right\}; p = 1, 2, 3, \quad (2)$$

$$W_{z4}(\omega) = (1/4) \left\{ W_{R4}(\omega - \omega_r) + W_{R4}(\omega + \omega_r) \right\}. \quad (3)$$

The coefficients k_1 , k_2 , k_3 and k_4 in equation (1) are determined by the second-order moment and the fourth-order moment of the modulation data a_n and b_n (Appendix A). The first and second terms on the right hand side of (1) both correspond to the SS component. The third term corresponds to the SN component and the fourth term corresponds to the NN component. Each component can be represented by the equations (2) and (3). It is shown the SS and SN component of jitter source PSD consist of 0th-order and ± 2 nd-order PSDs. $W_{R1}^{(k)}(\omega)$, $W_{R2}^{(k)}(\omega)$, and $W_{R3}^{(k)}(\omega)$, which are with respect to k th-order PSDs, and $W_{R4}(\omega)$ are shown in Appendix B.

The jitter PSD designated as $W_\phi(\omega)$ at the PLL output can be expressed as in equation (4).

$$W_\phi(\omega) = (2/A_S)^2 |H(\omega)|^2 W_z(\omega), \quad (4)$$

where $H(\omega)$ is the PLL closed loop transfer function and $W_z(\omega)$, given in (1), is related to the source of jitter generation and is thus referred to as the jitter source PSD at the squarer output here. The jitter PSD can then be represented as in equation (5), as the sum of the SS, SN and NN component, which are respectively given in equations (6) through (8).

$$W_\phi(\omega) = W_{\phi SS}(\omega) + W_{\phi SN}(\omega) + W_{\phi NN}(\omega), \quad (5)$$

$$W_{\phi SS}(\omega) = K_1 |H(\omega)|^2 W_{z1}(\omega) + K_2 |H(\omega)|^2 W_{z2}(\omega), \quad (6)$$

$$K_1 = (2/A_S)^2 k_1, \quad K_2 = (2/A_S)^2 k_2,$$

$$W_{\phi SN}(\omega) = K_3 |H(\omega)|^2 W_{z3}(\omega), \quad K_3 = (2/A_S)^2 k_3, \quad (7)$$

$$W_{\phi NN}(\omega) = K_4 |H(\omega)|^2 W_{z4}(\omega), \quad K_4 = (2/A_S)^2 k_4, \quad (8)$$

where

$$A_S = M_2 A_T / T \quad (\text{ASK}), \quad (9)$$

$$A_S = 2M_2 A_T / T \quad (\text{PAM, QAM}), \quad (10)$$

$$A_T = |G_a(\omega_r)|, \quad (11)$$

$$M_2 = (M^2 - 1)/3. \quad (12)$$

Here, $G_a(\omega)$ in equation (11) is the spectrum of $g^2(t)$, where $g(t)$ is the signal waveform at the receive filter output. M_2 , given in equation (12), is the second-order moment of modulation data, where M is an alphabet size.

The sum of $K_1 W_{z1}(\omega)$ and $K_2 W_{z2}(\omega)$ terms appearing in equation (6) make up the SS component of the jitter source PSD at the squarer output, $K_3 W_{z3}(\omega)$ in equation (7) is the SN component of the jitter source PSD, and $K_4 W_{z4}(\omega)$ in equation (8) is the NN component of the jitter source PSD.

As shown in equation (13), the jitter variance is given as the sum of the SS, SN, and NN components, which are given in equations (14), (15), and (16), respectively.

$$\sigma_\phi^2 = \sigma_{\phi SS}^2 + \sigma_{\phi SN}^2 + \sigma_{\phi NN}^2, \quad (13)$$

$$\sigma_{\phi SS}^2 = (1/2\pi) \int_{-\infty}^{\infty} W_{\phi SS}(\omega) d\omega, \quad (14)$$

$$\sigma_{\phi SN}^2 = (1/2\pi) \int_{-\infty}^{\infty} W_{\phi SN}(\omega) d\omega, \quad (15)$$

$$\sigma_{\phi NN}^2 = (1/2\pi) \int_{-\infty}^{\infty} W_{\phi NN}(\omega) d\omega. \quad (16)$$

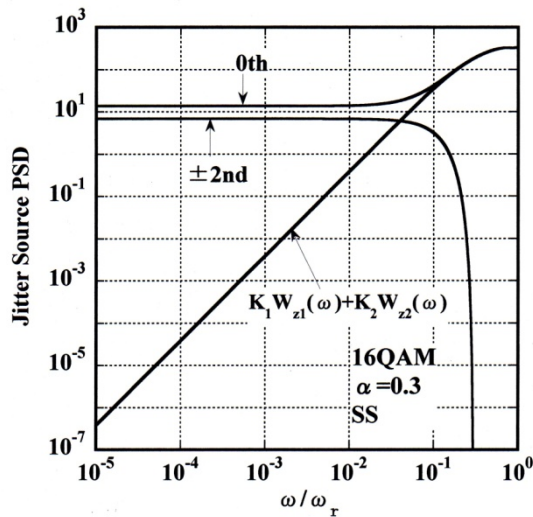
IV. NUMERICALLY CALCULATED RESULTS

A. SS Component

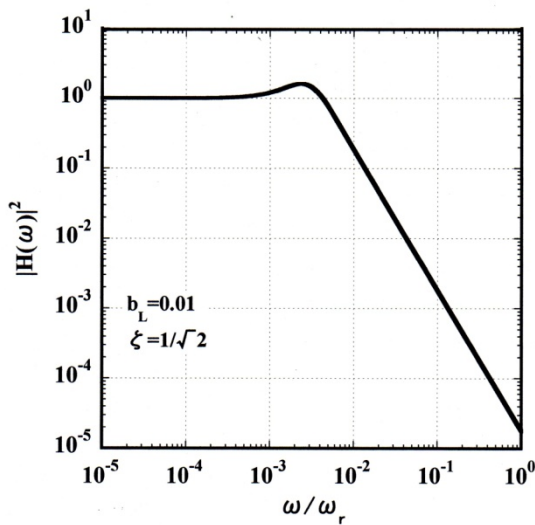
Figure 2(a) shows the SS component of the jitter source PSD, $K_1 W_{z1}(\omega) + K_2 W_{z2}(\omega)$, at the squarer output with 16QAM and a roll-off factor of 0.3. Also shown are the 0th-order PSD and ± 2 nd-order PSDs. The +2nd- and -2nd-order PSDs are identical. The jitter source PSD is the difference between the 0th-order PSD and the ± 2 nd-order PSDs as given in equation (2). Thus, as a result, the jitter source PSD is proportional to the square of ω/ω_r when ω/ω_r is less than 10^{-1} . The effect of the ± 2 nd-order PSDs, as well as that of the 0th-order PSD, on the SS component of the jitter source PSD is explicitly demonstrated.

Figure 2(b) shows the PLL transfer characteristics with a PLL normalized noise bandwidth b_L of 0.01 and a damping factor of $1/\sqrt{2}$.

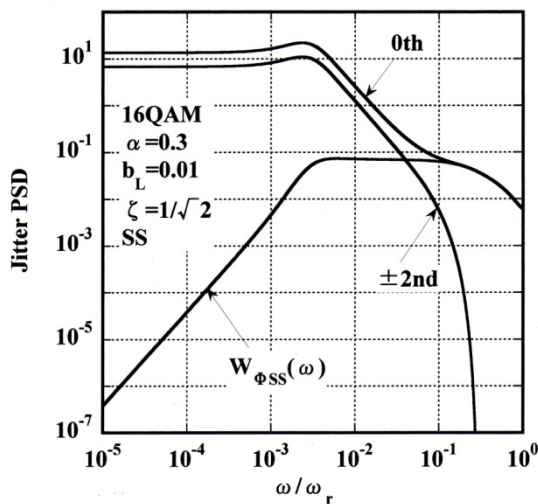
Figure 2(c) shows the SS component of the jitter PSD, $W_{\phi SS}(\omega)$, at the PLL output. Also shown are the 0th- and ± 2 nd-order PSDs, which are products of those shown in Figure 2(a) and the PLL transfer characteristics shown in Figure 2(b). Therefore, the +2nd- and -2nd-order PSDs are



(a) SS component of jitter source PSD



(b) PLL transfer characteristics



(c) SS component of jitter PSD

Figure 2. Spectral characteristics of SS component and PLL transfer characteristics.

identical. As shown, the jitter PSD within the PLL bandwidth is proportional to the square of ω/ω_r .

Figure 3 shows the SS component of jitter variance, $\sigma_{\phi SS}^2$, as a function of b_L . Also shown are the jitter variances, designated as 0th and $\pm 2nd$, due to the frequency integration of the 0th- and $\pm 2nd$ -order PSDs in Figure 2(c), respectively. $\sigma_{\phi SS}^2$ is obtained as the difference between the 0th and $\pm 2nd$ variances and is proportional to b_L^2 as presented in [6]-[8]. The 0th- and $\pm 2nd$ jitter variances themselves are proportional to b_L . Thus, if only the 0th-order PSD is assumed to exist, jitter variance is overestimated. Therefore, the effect of $\pm 2nd$ -order PSDs on the SS component of the jitter variance is explicitly presented as shown in Fig.3.

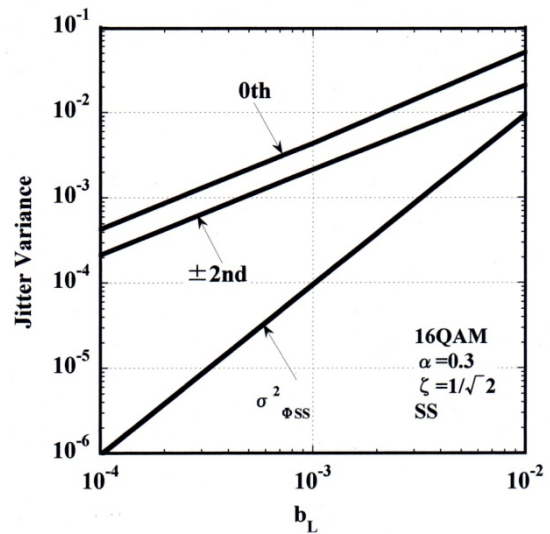
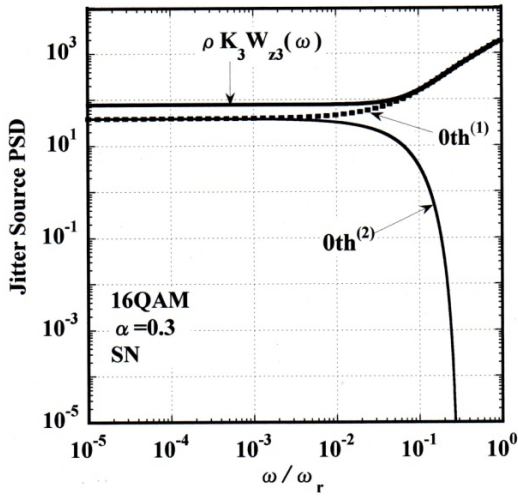


Figure 3. SS component of jitter variance as a function of b_L .

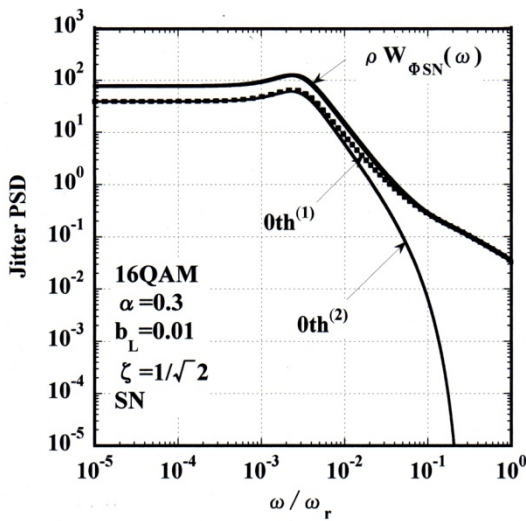
B. SN Component

Figure 4(a) shows the SN component of the jitter source PSD normalized by ρ , $\rho K_3 W_{z3}(\omega)$, at the squarer output, where ρ is the SNR at the receive filter output. Also shown are the 0th-order PSDs. These are designated as 0th⁽¹⁾ and 0th⁽²⁾ and correspond to the first term, $W_{R3}^{(0)}(\omega - \omega_r)$, and the second term, $W_{R3}^{(0)}(\omega + \omega_r)$, respectively, on the right-hand side of equation (2). Numerical calculation reveals that the $\pm 2nd$ -order PSDs are 0. This may be considered to be due to the band-limiting scheme assumed herein. Thus, the SN component of the jitter source PSD is given by the sum of the 0th⁽¹⁾ and 0th⁽²⁾ PSDs. When ω/ω_r is less than 10^{-2} , the two PSDs are almost identical with flat characteristics.

Figure 4(b) shows the normalized jitter PSD at the PLL output, $\rho W_{\phi SN}(\omega)$. Also shown are the 0th⁽¹⁾ and 0th⁽²⁾ PSDs. These PSDs are the product of the PSDs shown in Figure 4(a) and the PLL transfer characteristics. As shown, the SN component may be regarded as a stationary random process in the case of the band-limiting scheme assumed herein.



(a) SN component of jitter source PSD



(b) SN component of jitter PSD

Figure 4. SN component of spectral characteristics

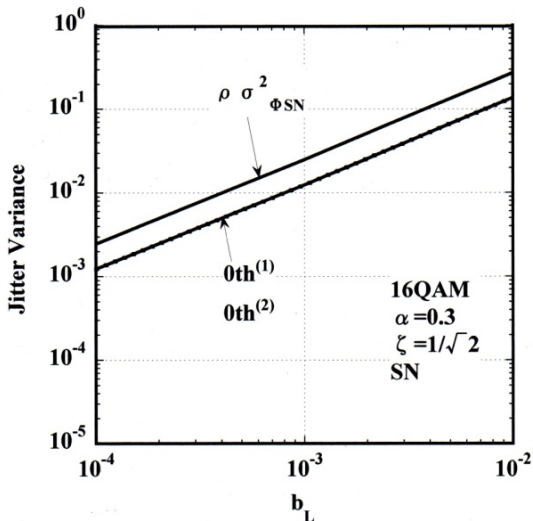
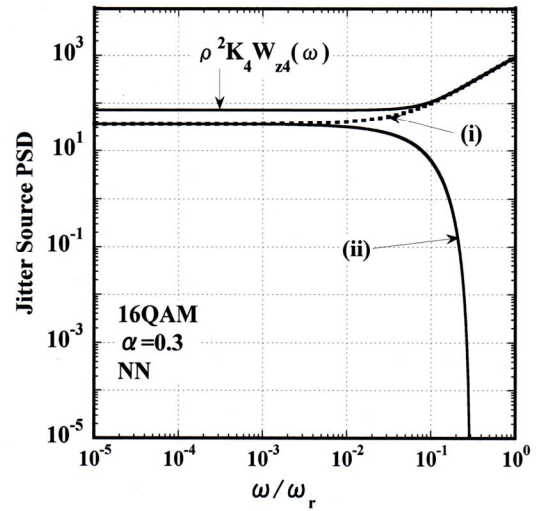
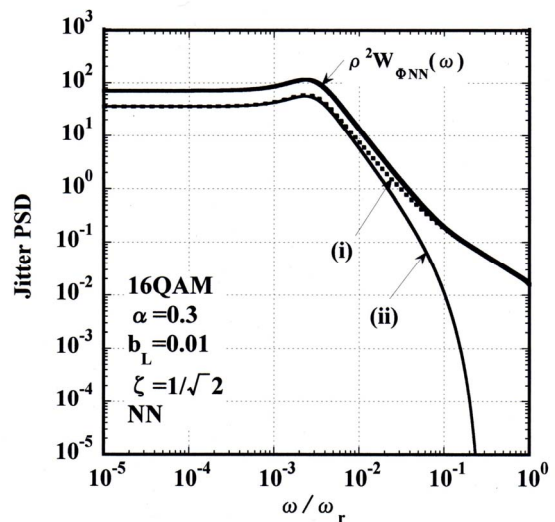


Figure 5. SN component of jitter variance as a function of b_L

Figure 5 shows the normalized SN component of the jitter variance, $\rho \sigma_{\phi_{SN}}^2$, as a function of b_L . Also shown are the jitter variances designated as $0th^{(1)}$ and $0th^{(2)}$ due to the frequency integration of $0th^{(1)}$ and $0th^{(2)}$ PSDs shown in Figure 4(b) over the finite frequency domain. $0th^{(1)}$ and $0th^{(2)}$ are identical. This is because the $0th^{(1)}$ PSD in the negative frequency domain is the mirror image of the $0th^{(2)}$ PSD in the positive frequency domain. Similarly, the $0th^{(2)}$ PSD in the negative frequency domain is the mirror image of the $0th^{(1)}$ PSD in the positive frequency domain. In [6] and [7], the SN component of the jitter variance was shown to be proportional to b_L ; here, we show that both the $0th^{(1)}$ and $0th^{(2)}$ jitter variances are also proportional to b_L .



(a) NN component of jitter source PSD



(b) NN component of jitter PSD

Figure 6. NN component of jitter spectral characteristics.

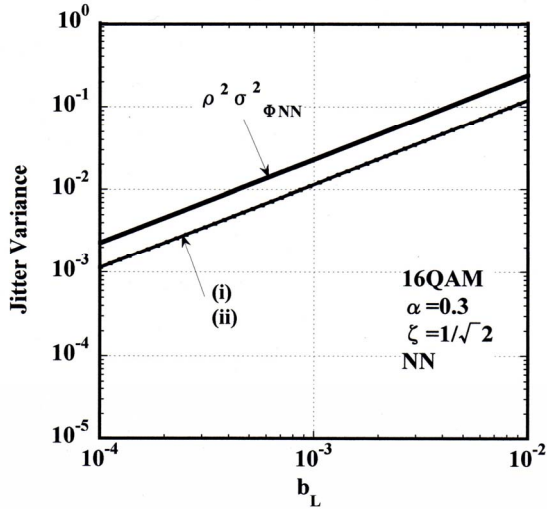


Figure 7. NN component of jitter variance as a function of b_L .

C. NN Component

Figure 6(a) shows the normalized NN component of the jitter source PSD, $\rho^2 K_4 W_{z4}(\omega)$, at the squarer output. The PSDs designated as (i) and (ii) in the figure exhibit PSDs corresponding to the first term and the second term on the right-hand side of equation (3). Because the NN component originates from white Gaussian noise, the higher-order PSDs do not exist. Therefore, the NN component has been calculated as a stationary random process.

Figure 6(b) shows the normalized NN component of the jitter PSD, $\rho^2 W_{\phi NN}(\omega)$, at the PLL output. The jitter PSD is given as the product of PSDs shown in Figure 6(a) and the PLL transfer characteristics.

Figure 7 shows the normalized NN component of jitter variance, $\rho^2 \sigma_{\phi NN}^2$, as a function of b_L . Also shown are the first and second terms on the right-hand side of equation (3), designated as (i) and (ii), respectively. As shown, (i) and (ii) are identical and proportional to b_L .

From the results presented in [7] and [8], the system design parameters such as the alphabet size, M , the SNR, ρ , the PLL normalized noise bandwidth, b_L , and the roll-off factor, α , are considered to be independent with each other. Therefore, the effect of higher-order PSDs on jitter variance presented herein holds for any transmission scheme, any values of M , ρ , and α treated herein.

V. CONCLUSIONS

Theoretical calculation reveals that the SS and SN components of the jitter source PSD at the squarer output consist of the 0th- and the ± 2 nd-order PSDs. Also clearly demonstrated is that the SS component of the jitter variance is overestimated if only the 0th-order PSD is taken into account. Numerical calculation shows that the SN component of the jitter variance consists of only 0th-order jitter variance because the ± 2 nd-order PSD is zero. This is due to the

band-limiting scheme assumed herein. Thus, the SN component of the jitter variance may be obtained by regarding the component as a stationary random process. Because the NN component originates from additive white Gaussian noise, the higher-order PSDs do not exist.

The results obtained in this paper are expected to be useful for evaluating jitter generation mechanism.

We would like to examine the effect of timing jitter on the symbol error rate in the future.

ACKNOWLEDGEMENT

The authors would like to thank Professor Kazuhiro Miyauchi for his valuable guidance and suggestions regarding this study.

REFERENCES

- [1] F. M. Gardner, "Self-noise in synchronizers," *IEEE Trans. Commun.*, vol.COM-28, pp.1159-1163, August 1980.
- [2] M. Moeneclaye, "Linear phase-locked loop theory for cyclostationary input disturbances," *IEEE Trans. Commun.*, vol.COM-30, NO.10, pp.2253-2259, October 1982.
- [3] E. Panayirci, "Analysis of self-noise in a clock recovery system with a high-order nonlinearity," *IEEE Trans. on Information Theory*, vol.49, no.11, pp.3106-3116, Nov. 2003.
- [4] J. A. Lopez-Salcedo, G. Vazquez, "Asymptotic equivalence between the unconditional maximum likelihood and the square-law nonlinearity symbol timing estimation," *IEEE Trans. Signal Processing*, vol.54, no.1, pp.244-257, Jan. 2006.
- [5] K. Miyauchi, I. Wakabayashi and H. Shibayama, "Analysis of timing jitter in digital transmission systems," *IEICE Trans. Commun. (Japanese ed.)*, vol.J83-B, no.5, pp.654-665, May 2000.
- [6] K. Miyauchi, I. Wakabayashi, "Analysis of timing jitter in PAM, ASK and QAM," *IEICE Trans. Commun. (Japanese ed.)*, vol.J93-B, no.8, pp.1051-1060, Aug. 2010.
- [7] I. Wakabayashi, "Timing jitter in PAM, ASK, and QAM for a bandlimiting scheme," in *12th Proceedings of ICACT2010*, pp.318-323, Feb. 2010.
- [8] I. Wakabayashi, S. Urano, and M. Sano, "Dependency of jitter variance on PLL normalized noise bandwidth," in *13th Proceedings of ICACT2011*, pp.1-6, Feb. 2011.
- [9] S. Urano, I. Wakabayashi, M. Sano, "Effect of a pre-filter on timing jitter," in *14th Proceedings of ICACT2013*, pp.132-137, Feb. 2012.

APPENDIX

A. The coefficients $k_1, k_2, k_3,$ and k_4

$$W_z(\omega) = k_1 W_{z1}(\omega) + k_2 W_{z2}(\omega) + k_3 W_{z3}(\omega) + k_4 W_{z4}(\omega) \quad (\text{A.1})$$

$$k_1 = M_2^2, \quad k_2 = (3M_2^2 - M_4)/2, \quad k_3 = M_2, \quad k_4 = 1 \quad (\text{PAM}) \quad (\text{A.2})$$

$$k_1 = M_2^2/4, \quad k_2 = (3M_2^2 - M_4)/8, \quad k_3 = M_2/4, \quad k_4 = 1/2 \quad (\text{ASK}) \quad (\text{A.3})$$

$$k_1 = M_2^2/2, \quad k_2 = (3M_2^2 - M_4)/4, \quad k_3 = M_2/2, \quad k_4 = 1/2 \quad (\text{QAM}) \quad (\text{A.4})$$

$$M_2 = (M^2 - 1)/3 \quad (\text{A.5})$$

$$M_4 = (M^2 - 1)(3M^2 - 7)/15 \quad (\text{A.6})$$

where M_2 and M_4 are the second- and the fourth-order moment of modulation data a_n and b_n , and M is the alphabet size.

B. PSDs of $W_{R1}^{(k)}(\omega)$, $W_{R2}^{(k)}(\omega)$, $W_{R3}^{(k)}(\omega)$, and $W_{R4}(\omega)$

$$W_{R1}^{(k)}(\omega) = \frac{1}{\pi T^2} \sum_{n=-\infty}^{\infty} \int_{-\infty}^{\infty} G(x)G(n\omega_r - x)G(\omega - x) \times G((k-n)\omega_r - \omega + x)dx \quad (\text{B.1})$$

$$W_{R2}^{(k)}(\omega) = -2T^{-1}G_a(\omega)G_a(k\omega_r - \omega) \quad (\text{B.2})$$

$$W_{R3}^{(k)}(\omega) = 2(\pi T)^{-1} \int_{-\infty}^{\infty} G(x)G(k\omega_r - x)G_v(\omega - x)dx \quad (\text{B.3})$$

$$W_{R4}(\omega) = \frac{\lambda^2 N_0^2}{\pi} \int_{-\infty}^{\infty} |G_R(x)|^2 |G_R(\omega - x)|^2 dx \quad (\text{B.4})$$

where

$$\lambda = 1/2 \text{ (PAM)}, \quad \lambda = 1 \text{ (ASK, QAM)} \quad (\text{B.5})$$

$$G(\omega) = G_T(\omega)G_R(\omega) \quad (\text{B.6})$$

$$G_a(\omega) = \frac{1}{2\pi} \int_{-\infty}^{\infty} G(x)G(\omega - x)dx \quad (\text{B.7})$$

$$G_v(\omega) = (N_0/2)|G_R(\omega)|^2 \text{ (PAM)} \quad (\text{B.8})$$

$$G_v(\omega) = N_0|G_R(\omega)|^2 \text{ (ASK, QAM)} \quad (\text{B.9})$$

Here, $G(\omega)$ is the Fourier transformation of the receive filter output waveform $g(t)$ as shown in equation (B.6) and it is assumed to be of a cosine roll-off, where $G_T(\omega)$ and $G_R(\omega)$ are the frequency spectrum of the transmit pulse waveform and the receive filter transfer function, respectively. $G_a(\omega)$ is the Fourier transformation of $g^2(t)$ and is expressed in equation (B.7). $G_v(\omega)$ is PSD of Gaussian noise at the receive filter output and is defined in equations (B.8) and (B.9).